International Journal of the Physical Sciences Vol. 6(19), pp. 4533-4547, 16 September, 2011
Available online at http://www.academicjournals.org/IJPS
DOI: 10.5897/IJPS11.757
ISSN 1992 - 1950 ©2011 Academic Journals

Full Length Research Paper

Capability measures for Weibull processes with mean shift based on Erto's-Weibull control chart

Ya-Chen Hsu[1]*, W. L. Pearn[2] and Chun-Seng Lu[2]

[1]Department of Business Administration, Yuanpei University, Taiwan, ROC.
[2]Department of Industrial Engineering and Management, National Chiao Tung University, Taiwan, ROC.

Accepted 5 August, 2011

Process capability indices (PCIs), which are effective tools for quality assurance and are guidance for process improvement, have been proposed in the manufacturing industry to provide numerical measures on process reproduction capability. PCIs are calculated under the assumption that the process is stable while the process mean and variation are not changeable. However, in practice, the process is dynamic. Under the Bothe's adjustments, we showed the detection powers of the percentile-Weibull control chart, bootstrap-Weibull control chart, and the Bayes-Weibull control chart. It is realized that the Bothe's adjustments are inadequate with data coming from Weibull processes. For this reason, the PCIs have to be adjusted. Bothe (2002) provided the adjustment method for normality processes. In this research, we consider Weibull processes, which cover a wide class of applications. We calculate the mean shift adjustments under various sample sizes *n* and Weibull parameter γ, with the power fixed to 0.5. Then, we implement the adjustments to accurately estimate capability index C_{pk} for Weibull processes with mean shift consideration. Finally, an application example is presented for illustration purpose.

Key words: Dynamic C_{pk}, mean shift, process capability index, Weibull distribution, Weibull control chart.

INTRODUCTION

During the last decade, numerous process capability indices (PCIs) have been proposed in manufacturing industries to provide numerical measures on process performance. Production yield is one of the commonly used criteria for measuring process capability. Those indices are effective tools for process capability analysis and quality assurance. The relationship between the actual process performance and the specification limits or tolerance may be quantified by using appropriate process capability indices. Four basic well-known capability indices have been defined explicitly as follows (Kane, 1986; Chan et al., 1988; Pearn et al., 1992):

$$C_p = \frac{USL - LSL}{6\sigma}, \quad (1)$$

$$C_{pk} = \min\left\{\frac{USL-\mu}{3\sigma}, \frac{\mu - LSL}{3\sigma}\right\}, \quad (2)$$

$$C_{pm} = \frac{USL - LSL}{6\sqrt{\sigma^2 + (\mu - T)^2}}, \quad (3)$$

$$C_{pmk} = \min\left\{\frac{USL-\mu}{3\sqrt{\sigma^2 + (\mu - T)^2}}, \frac{\mu - LSL}{3\sqrt{\sigma^2 + (\mu - T)^2}}\right\}, \quad (4)$$

where USL is the upper limit and LSL is the lower specification limits, T is the target value, and μ and σ are, respectively, the process mean and the standard deviation of the characteristic.

In the literature, several authors have promoted the use of various process capability indices and examined their associated properties with different degrees of completeness.

Ever since Motorola, Inc. introduced its Six Sigma quality initiative, followers of this philosophy notion should add a shift to the process average before estimating process capability. The advocates of the six sigma production quality have claimed that such an adjustment is necessary, but they have offered only personal

*Corresponding author. E-mail: eujane27@gmail.com.

experiences and three dated empirical studies as justification for this claim (Bender, 1975; Evans, 1975; Gilson, 1951). Bothe (2002) first provided a statistically based reason to calculate the undetected shifts of various magnitudes, and then adjusted the formula of process capability. In Bothe's study, the process data is assumed to be approximately normally distributed. However, non-normal processes occur frequently, in particular, in the semiconductor industry. Hsu et al. (2008) investigated the procedure to calculate the mean shift adjustments for Gamma processes with power fixed to 0.5. Pyzdek (1992) mentioned that the distributions of certain chemical processes are very often skewed, such as zinc plating in a hot-dip galvanizing process. Choi et al. (1996) presented an example of a skewed distribution in the "active area" shaping stage of the wafer's production processes. Cygan et al. (1989) have mentioned that the lifetimes of polypropylene films under high ac and dc field stresses were shown as a two-parameter Weibull distribution. Weibull distribution denoted as Weibull $(\alpha,\ \gamma)$, with various values of α and γ, covers a wide class of non-normal processes, including product life, product reliability and tensile strength of brittle materials, such as carbon, and boron. Since many other processes could be modeled by Weibull distributions, we determine the adjustments for capability measurements with the mean shift consideration for Weibull processes in this paper.

The control charts are commonly used in many industries for providing early warnings of the shift in the process mean. The well-known Shewhart $\bar{X}$ control chart is developed based on the assumption that the process data is normally distributed. When the process data is from a Weibull distribution, the estimators of the sampling-distribution parameters may not be available theoretically. For Weibull processes, Erto and Pallotta (2007) used Bayes theorem to provide a Weibull control chart. Nichols and Padgett (2006) provided a bootstrap-Weibull control chart for Weibull processes. Lu and Peng (2003) found the approximate c.d.f. of $\bar{X}_n$ ($\bar{X}_n = \frac{1}{n}\sum_{i=1}^{n} X_i$, X_1 , X_2 ,....., X_n be sequence observations of *i.i.d* Weibull $(1,\ \gamma)$) distribution to provide a percentile control chart for the calculations of the control limits, LCL and UCL. This paper first shows the detection power of the three control charts (Erto's-Weibull control chart provided by Erto and Pallotta (2007), bootstrap-Weibull control chart provided by Nichols and Padgett (2006) and percentile-Weibull control chart provided by Lu and Peng (2003)) under the Bothe's mean shift adjustments. For the three control charts, the low detection power shows that Bothe's adjustments are inadequate when the process is Weibull distributed. Then, we use the most powerful control chart of the three ones to estimate the adjustments under various sample sizes (*n*) and Weibull parameters (γ) with a fixed detection power of 0.5. Finally, the process capability formula is adjusted to accommodate the undetected shifts. As a result, our adjustments significantly provide more accurate calculations of the capability in the Weibull processes. A real-world example taken from the manufacturing process is investigated to illustrate the applicability of the process capability index.

WEIBULL PROCESS

Since Weibull distribution has often been used in the field of life data analysis due to its flexibility, and it can mimic the behaviors of other statistical distributions such as the normal and the exponential. We choose Weibull distributions to model the data of the processes in this research. Weibull distributions are also used to model the time until a given technical device fails.

Weibull distribution

Weibull distribution is the non-negative distribution. It can be denoted as Weibull ($\alpha,\ \gamma$) with scale parameter α and shape parameter γ. The cumulative density function is defined as

$$F(X) = 1\text{-}e^{-(x/a)^{\gamma}},\ x>0,\ \alpha>0,\ \gamma>0, \tag{5}$$

and the probability density is

$$f(x) = \gamma\alpha^{-\gamma}x^{\gamma-1}e^{-(\frac{x}{\alpha})^{\gamma}},\ x>0,\ \alpha>0,\ \gamma>0, \tag{6}$$

The mean and variance are respectively given by

$$\mu = \alpha[\Gamma(1+\gamma^{-1})], \tag{7}$$

and

$$\sigma^2 = \alpha^2[\Gamma(1+2\gamma^{-1}) - \Gamma^2(1+\gamma^{-1})]. \tag{8}$$

The coefficient of skewness Weibull distribution is given by:

$$\gamma_1 = \frac{2\Gamma^3(1+\gamma^{-1}) - 3\Gamma(1+\gamma^{-1})\Gamma(1+2\gamma^{-1}) + \Gamma(1+3\gamma^{-1})}{[\Gamma(1+2\gamma^{-1}) - \Gamma^2(1+\gamma^{-1})]^{3/2}}. \tag{9}$$

The kurtosis coefficient of Weibull distribution is given by:

$$\gamma_2 = \frac{f(\gamma)}{[\Gamma(1+2\gamma^{-1}) - \Gamma^2(1+\gamma^{-1})]^2}, \tag{10}$$

Where $\Gamma(x)$ is the gamma function and

Table 1. Values of skewness and kurtosis of various Weibull distributions.

Weibull(α, γ)	Skewness	Kurtosis
Normal(0,1)	0	0
Weibull(1,1)	2	6
Weibull(1,2)	0.631111	0.245089
Weibull(1,3)	0.168103	-0.27054
Weibull(1,3.6)	0	-0.283255
Weibull(1,4)	-0.087237	-0.25217
Weibull(1,5)	-0.25411	-0.11971
Weibull(1,6)	-0.373262	0.035455
Weibull(1,7)	-0.46319	0.187183
Weibull(1,8)	-0.533726	0.327676
Weibull(1,9)	-0.590657	0.455204
Weibull(1,10)	-0.637637	0.570166

$$f(\gamma) \equiv -6\Gamma^{-4}(1+\gamma^{-1}) + 12\Gamma^{-2}(1+\gamma^{-1})\Gamma(1+2\gamma^{-1}) - 3\Gamma^{-2}(1+2\gamma^{-1}) - 4\Gamma(1+\gamma^{-1})\Gamma(1+3\gamma^{-1}) + \Gamma(1+4\gamma^{-1}). \quad (11)$$

The Equations (9) and (10) show that the skewness coefficient and the kurtosis coefficient are calculated only by using the shape parameter γ, which means that the scale parameter α can not affect the values of skewness and kurtosis of Weibull distributions. Therefore, we fix $\alpha = 1$ in this study for the Weibull distributions. To see how this distribution are different from the standard normal distribution in terms of skewness and kurtosis, Table 1 shows the values of skewness and kurtosis (which are respectively defined as the third and the fourth moments of the standardized distribution) of the Weibull distributions under study. Also, when the value of γ increases from 1 to 3.6, the corresponding values of skewness will become smaller and will be close to 0. Especially, when value of γ is 3.6, the skewness coefficient of the Weibull distribution is 0, indicating that the Weibull (1, 3.6) distribution is symmetric about median and appears more nearly normal distribution. When the value of γ increases form 3.6 to 10, the corresponding values of skewness will become negative and far from 0. Based on the results above, we can get some insights of the effects of non-normality in terms of skewness and kurtosis.

The formula of these modulus let us know that α is the scale parameter and γ is the shape parameter. It can be seen that as the value of γ in the region of [3, 4], the skewness and kurtosis of Weibull distribution will be getting much closer to those of normal distribution. In this study, without the loss of generality, we let $\gamma =$ 1(1)10, while fixing $\alpha = 1$. This fact could also be found according to Equation (10). When the value of γ in the region of of [3, 4], the form of Weibull distribution becomes centralizing. Through these distributions, we expect to get some insights of the effects of non-normality on the detection power in terms of skewness and kurtosis. Through these distributions, we expect to get some insights of the effects of non-normality on the detection power in terms of skewness and kurtosis.

The detection power of the percentile-Weibull control chart

Here, we use percentile-Weibull control chart to calculate the detection power. Let $X_1, X_2, \ldots, X_n$ be a sequence observations of independent and identically distributed in Weibull (α, γ). The detection power is defined the probability of outline control chart under the mean being shifted. Its mean 1-type □ error β. The detection power is:

$$\begin{aligned} \text{Detection power} &= 1\text{-}P(LCL \le \bar{X}_n \le UCL \,|\, \mu_1 = \mu_0 + k\sigma_x) \\ &= 1\text{-}P(F_{\bar{X}(0.00135)} \le \bar{X}_n \le F_{\bar{X}(0.99865)} \,|\, \mu_1 = \mu_0 + k\sigma_x), \end{aligned} \quad (12)$$

where μ_1 is the mean after process shift (μ_0 is the mean of the original process). The control limits LCL and UCL are calculated as $F_{\bar{X}_n(0.00135)}$ and $F_{\bar{X}_n(0.99865)}$ respectively, where $F_{\bar{X}_n(0.00135)}$ and $F_{\bar{X}_n(0.99865)}$ are 0.135th percentile and 99.865th of $\bar{X}$ of sampling distribution. We can obtain the approximate c.d.f. of $\bar{X}_n$ distribution by a reference which Lu and Peng (2003) provided. Since the $\bar{X}_n$ distribution is not symmetric, we discussed μ occurred right movement and left movement. When $k > 0$, μ occurs right movement; and when $k < 0$, μ occurs left movement. Tables 2 and 3 display the detection power with right process mean shift ($k > 0$) and left process mean shift ($k < 0$) when $X_1, X_2, \ldots, X_n$ come from Weibull (α, γ) with $\alpha = 1$ and $\gamma = 1\ (1)\ 10$, and the number of subgroup is 100000. The magnitude of shift in the second column on the left is Bothe's capability adjustments determined when data comes from normal distribution and the detection power is 0.5. In Table 2, we can see that the detection power is less than 0.5 when $\gamma = 1$ and 2 while, in Table 3, $\gamma \ge 5$ under Bothe's capability adjustments. The results indicate that the Bothe's adjustments are inadequate when we have Weibull processes due to Bothe's approach which is based on the normality assumption of the data and the

Table 2. Detection power of the percentile-Weibull control chart for $k > 0$ under various Weibull distributions.

n	Shift σ	Weibull distribution(1, γ) for right shift									
		γ=1	γ=2	γ=3	γ=4	γ=5	γ=6	γ=7	γ=8	γ=9	γ=10
2	2.12	0.054	0.309	0.525	0.687	0.747	0.785	0.807	0.822	0.833	0.841
3	1.73	0.091	0.347	0.524	0.664	0.726	0.760	0.782	0.796	0.809	0.815
4	1.5	0.099	0.375	0.516	0.646	0.699	0.735	0.756	0.775	0.784	0.793
5	1.34	0.119	0.378	0.514	0.626	0.681	0.712	0.738	0.752	0.764	0.775
6	1.22	0.141	0.389	0.509	0.614	0.668	0.696	0.719	0.734	0.747	0.755
7	1.13	0.149	0.385	0.517	0.596	0.645	0.677	0.699	0.715	0.728	0.737
8	1.06	0.163	0.391	0.516	0.589	0.636	0.666	0.688	0.704	0.717	0.726
9	1.00	0.175	0.398	0.513	0.582	0.626	0.656	0.678	0.693	0.705	0.714
10	0.95	0.188	0.403	0.512	0.577	0.620	0.648	0.668	0.684	0.695	0.705

Table 3. Detection power of the percentile-Weibull control chart for $k < 0$ under various Weibull distributions.

n	Shift σ	Weibull distribution(1, γ) for left shift									
		γ=1	γ=2	γ=3	γ=4	γ=5	γ=6	γ=7	γ=8	γ=9	γ=10
2	2.12	0.928	0.782	0.550	0.513	0.439	0.387	0.350	0.323	0.304	0.288
3	1.73	0.906	0.733	0.537	0.506	0.449	0.411	0.384	0.364	0.348	0.337
4	1.5	0.886	0.702	0.532	0.505	0.458	0.426	0.404	0.385	0.375	0.365
5	1.34	0.868	0.680	0.527	0.504	0.464	0.436	0.416	0.401	0.390	0.381
6	1.22	0.852	0.664	0.525	0.504	0.467	0.441	0.424	0.411	0.401	0.393
7	1.13	0.836	0.649	0.553	0.499	0.466	0.443	0.427	0.416	0.406	0.399
8	1.06	0.825	0.642	0.552	0.502	0.471	0.450	0.436	0.424	0.416	0.409
9	1.00	0.814	0.634	0.549	0.503	0.474	0.454	0.440	0.430	0.422	0.415
10	0.95	0.805	0.629	0.548	0.504	0.477	0.458	0.445	0.435	0.427	0.421

detection power is 0.5. In Tables 2 and 3, the detection power is more than 0.5 when $\gamma = 3$ and 4. This means that Weibull distribution is close to normal distribution when $\gamma = 3$ and 4. This fact could also be found from Table 1. As the value of γ in the region of [3, 4], the form of Weibull distribution becomes centralizing. However, the detection power is poorer and far less than 0.5 when data comes more from skewed Weibull distribution. For example, when $\gamma = 1$ and the subgroup size $n = 2$, the detection power is 0.054. It implies that Bothe's adjustments are inadequate when we have skewed processes. Consequently, in our study, we determine the capability adjustment when process data comes from Weibull distribution.

The detection power of the bootstrap-Weibull control chart

The usual Shewhart control charts assume that the observed process data come from a near-normal distribution. However, when the distribution of the process under observation is unknown or non-normal such as Gamma or Weibull, the sampling distribution of a parameter estimator may not be available theoretically. One way to estimate parameter is simulation. Nichols and Padgett (2006) provided a bootstrap-Weibull control chart for Weibull percentiles. This control chart uses bootstrap method to construct control chart limits for monitoring a specified percentile of the process distribution.

The percentile of the Weibull distribution is

$$W_p = \alpha[-\ln(1-p)]^{\frac{1}{\gamma}}, \quad 0 < p < 1,$$

where W_p is the 100 p th percentile.

The following steps are used to construct the bootstrap-Weibull control chart.

1. Let x_{ij}, $i = 1,\ldots,n,$ and $j = 1,\ldots,m,$ be the observations assumed to come from m independent subgroups of size n and distributed in Weibull (α, γ).

2. Using the maximum likelihood method to find $\hat{\alpha}$ and

Table 4. Detection power of the bootstrap-Weibull control chart for $k > 0$ under various Weibull distributions.

n	hift σ	Weibull distribution(1, γ) for right shift									
		γ=1	γ=2	γ=3	γ=4	γ=5	γ=6	γ=7	γ=8	γ=9	γ=10
2	2.12	0.066	0.283	0.489	0.572	0.642	0.679	0.717	0.733	0.755	0.758
3	1.73	0.118	0.306	0.456	0.574	0.644	0.669	0.702	0.710	0.721	0.743
4	1.5	0.180	0.329	0.476	0.574	0.617	0.646	0.666	0.698	0.716	0.727
5	1.34	0.169	0.355	0.461	0.543	0.603	0.638	0.669	0.673	0.688	0.722
6	1.22	0.256	0.344	0.488	0.541	0.581	0.626	0.661	0.674	0.697	0.704
7	1.13	0.289	0.363	0.488	0.538	0.581	0.618	0.652	0.676	0.678	0.705
8	1.06	0.305	0.381	0.470	0.538	0.592	0.616	0.656	0.659	0.682	0.691
9	1.00	0.343	0.384	0.480	0.547	0.581	0.612	0.643	0.656	0.676	0.688
10	0.95	0.361	0.395	0.491	0.552	0.580	0.634	0.640	0.658	0.682	0.683

Table 5. Detection power of the bootstrap-Weibull control chart for $k < 0$ under various Weibull distributions.

n	Shift σ	Weibull distribution(1, γ) for right shift									
		γ=1	γ=2	γ=3	γ=4	γ=5	γ=6	γ=7	γ=8	γ=9	γ=10
2	2.12	0.955	0.795	0.627	0.512	0.440	0.388	0.359	0.334	0.319	0.289
3	1.73	0.953	0.755	0.592	0.499	0.464	0.419	0.385	0.374	0.362	0.340
4	1.5	0.952	0.726	0.582	0.496	0.462	0.431	0.391	0.385	0.409	0.385
5	1.34	0.949	0.707	0.554	0.509	0.465	0.441	0.437	0.434	0.415	0.407
6	1.22	0.947	0.692	0.574	0.518	0.466	0.482	0.435	0.440	0.434	0.432
7	1.13	0.946	0.676	0.561	0.494	0.483	0.445	0.466	0.446	0.452	0.456
8	1.06	0.946	0.667	0.533	0.490	0.480	0.467	0.465	0.442	0.442	0.445
9	1.00	0.942	0.663	0.559	0.484	0.494	0.455	0.456	0.452	0.427	0.469
10	0.95	0.943	0.662	0.544	0.511	0.488	0.482	0.492	0.454	0.459	0.473

$\hat{\gamma}$. The equations are

$$\gamma=\left[\frac{\sum_{j=1}^{m}\sum_{i=1}^{n}x_{ij}^{\gamma}\ln x_i}{\sum_{j=1}^{m}\sum_{i=1}^{n}x_{ij}^{\gamma}}-\frac{\sum_{j=1}^{m}\sum_{i=1}^{n}x_{ij}^{\gamma}\ln x_i}{nm}\right]^{-1} \text{ and } \alpha=\left[\frac{\sum_{j=1}^{m}\sum_{i=1}^{n}x_{ij}^{\gamma}}{nm}\right]^{\frac{1}{\gamma}}.$$

3. Generate a bootstrap subgroup of size n, $x_1^*, x_2^*, \ldots x_n^*$, from the Weibull distribution using maximum likelihood estimators, $\hat{\alpha}$ and $\hat{\gamma}$, as the estimated parameters.

4. Find the parameter MLEs from the bootstrap subgroup and denote these as $\hat{\alpha}^*$ and $\hat{\gamma}^*$.

5. For the bootstrap subgroup, find $W_p = \hat{\alpha}^*[-\ln(1-p)]^{1/\hat{\gamma}^*}$, $0 < p < 1$, the bootstrap estimate of the 100 p th percentile, W_p.

6. Repeat steps 3 to 5 a large number of times, B, obtaining B bootstrap estimates of W_p, denoted by $W_{p1}^*, W_{p2}^*, \ldots, W_{pB}^*$.

7. Ordering the B bootstrap estimates W_{pi}^*, from smallest to largest to calculate the ($0.00135 \times B$) and the ($0.99865 \times B$) value of the ordered W_{pi}^* to be the LCL and UCL, respectively.

In order to calculate the detection power of the percentile-Weibull control chart, we set the percentile p=0.5 to make similar the sampling distribution of $\bar{X}_n$ and the repeated time B is 100000. Tables 4 and 5 indicate the detection power of the 50th percentile of the distribution with shift $k\sigma_x$ when data comes from Weibull distribution with the scale parameter $\alpha = 1$ and the shape parameter $\gamma = 1\ (1)\ 10$. The shift distance in the second column is Bothe's adjustment as the same as Tables 2 and 3. We can find that the detection power is less than 0.5 when $\gamma \leq 3$ in Table 4, and $\gamma \geq 5$ in Table 5. This results show that the Bothe's adjustments are inadequate when data comes from more skewed Weibull distribution, we have also the same results in the above section, that the detection power is poorer and far

less than 0.5.

Erto's-Weibull control chart for Weibull processes

Previously, we discussed that the Shewhart $\overline{\overline{X}}$ control chart assumed that the data should come from normal distribution. If data comes from non-normal distribution, such as Gamma or Weibull distribution, we just only use simulation or approximate to get an inexact results. In order to get an exact result, using a Weibull control chart which Erto and Pallotta (2007) provided is a better choice. Erto and Pallotta (2007) provided a new Shewhart-type control chart of Weibull percentile. We used Practical Bayes Estimators (PBE) of the Bayes theorem to integrate both technological and statistical information of the chart analytically. The PBE were developed from engineers' point of view.

The Weibull survival function is:

$$\mathrm{Sf}\{x;\alpha,\gamma\} = \exp\left[-(x/\alpha)^{\gamma}\right]; \qquad x \geq 0; \qquad \alpha,\gamma > 0, \tag{13}$$

where α, γ are the scale and shape parameters of the Weibull distribution. We can be immediately re-parameterized in terms of the percentile x_R and shape parameter β, in which the Engineers' knowledge can be more easily converted:

$$\mathrm{Sf}\{x;x_R,\gamma\} = \exp\left[-K(x/x_R)^{\gamma}\right], \quad x \geq 0, x_R, \quad \gamma > 0, \quad K = \ln(1/R), \tag{14}$$

where x_R and γ both being unknown. x_R is equivalent to the $1-R$ percentile of the Weibull distribution, for example, if $R = 0.90$ and $x_R = 1{,}000$ h, then 90% of the items have lives greater than 1,000 h. The uniform prior probability density function in the interval (γ_1, γ_2) is assumed to fit the degree of belief in the shape parameter β of the sampling distribution as:

$$\mathrm{pdf}\{\gamma\} = \begin{cases} 1/(\gamma_2 - \gamma_1); & \gamma_2 \geq \gamma \geq \gamma_1 > 0; \quad \gamma_2 > \gamma_1 \\ 0; \quad \text{elsewhere} \end{cases}, \tag{15}$$

and it appears to be as non-restrictive as feasible.

For the selected percentile x_R (corresponding to the fixed reliability level R) the prior probability density function is assumed to be the Inverse Weibull as follows:

$$\mathrm{pdf}\{x_R\} = a\,b\,(a\,x_R)^{-(b+1)} \exp\left[-(a\,x_R)^{-b}\right]; \qquad x_R \geq 0; \qquad a,b > 0, \tag{16}$$

where a and b are the scale and shape parameters respectively. It is assumed $b = \gamma$. When the the value of γ is larger, the peaked the Weibull probability density function is greater, and the uncertainty in x_R is smaller. In the meanwhile, b must be greater so that $b = \gamma$ would be the simplest choice. Thus, the probability density function of x_R is converted into the conditional prior as:

$$\mathrm{pdf}\{x_R|\gamma\} = a\,\gamma\,(a\,x_R)^{-(\gamma+1)} \exp\left[-(a\,x_R)^{-\gamma}\right]; \tag{17}$$

From Equation (15), the mean value $E\{x_R\}$ of the probability density function is $E\{x_R\} = (1/a)\ \Gamma(1-1/b)$. From this function, assuming $b = \gamma$, we know that

$$a = \frac{\Gamma(1-1/\gamma_m)}{E\{x_R\}}; \qquad \gamma_m = (\gamma_1 + \gamma_2)/2. \tag{18}$$

Usually, a sample array $\underline{x}$ of n experimental data is available. If the reliability of the items, measured in terms of lifetime, tensile strength, and breaking strength, etc., is characterized by the Equation (13), the likelihood of the sample is given by the following equation,

$$\mathrm{L}(\underline{x}|x_R,\gamma) \propto \left(\frac{\gamma}{x_R^{\gamma}}\right)^n \prod_{i=1}^{n} x_i^{\gamma-1} \ \exp\left(-\frac{K}{x_R^{\gamma}}\sum_{i=1}^{n} x_i^{\gamma}\right). \tag{19}$$

And from the two priors Equations (14) and (16), the joint probability density function of x_R and γ is obtained:

$$\mathrm{pdf}\{x_R,\gamma\} = (\gamma_2 - \gamma_1)^{-1}\, a\,\gamma\,(a\,x_R)^{-(\gamma+1)} \exp\left[-(a\,x_R)^{-\gamma}\right]. \tag{20}$$

Combining Equations (18) and (19) by using the Bayes theorem which substantially says,

$$\begin{pmatrix}\text{joint posterior probability density}\\ \text{of unknown parameters}\end{pmatrix} \propto \begin{pmatrix}\text{their joint prior}\\ \text{probability density}\end{pmatrix} \times \begin{pmatrix}\text{likelihood}\\ \text{function}\end{pmatrix}$$

"Prior" and "posterior" respectively indicate the time before and after obtaining the experimental data. Therefore, in this way, the theorem fuses the technological prior knowledge, summarized into the joint prior, with all the information, including data and the shape of the reliability model, into likelihood. We can get the joint posterior probability density function of unknown parameters as follows,

Table 6. Detection power of the Erto's-Weibull control chart for $k > 0$ under various Weibull distributions.

n	Shift σ	Weibull distribution(1, γ) for right shift									
		γ=1	γ=2	γ=3	γ=4	γ=5	γ=6	γ=7	γ=8	γ=9	γ=10
2	2.12	0.276	0.649	0.823	0.861	0.906	0.937	0.949	0.955	0.964	0.974
3	1.73	0.345	0.615	0.736	0.826	0.841	0.871	0.894	0.899	0.914	0.920
4	1.5	0.454	0.598	0.715	0.778	0.838	0.844	0.861	0.873	0.883	0.890
5	1.34	0.477	0.588	0.704	0.753	0.806	0.828	0.841	0.859	0.865	0.869
6	1.22	0.539	0.579	0.686	0.735	0.770	0.803	0.818	0.834	0.840	0.858
7	1.13	0.589	0.602	0.679	0.727	0.769	0.784	0.812	0.830	0.831	0.849
8	1.06	0.603	0.607	0.680	0.728	0.763	0.790	0.812	0.827	0.835	0.844
9	1.00	0.648	0.591	0.656	0.720	0.761	0.781	0.795	0.805	0.822	0.830
10	0.95	0.656	0.580	0.667	0.715	0.750	0.779	0.796	0.805	0.827	0.830

$$\text{pdf}\{x_R, \gamma \mid \underline{x}\} = \frac{\gamma^{n+1} a^{-\gamma} x_R^{-\gamma(n+1)-1} \prod_{i=1}^{n} x_i^{\gamma-1} \exp\left[-x_R^{-\gamma}\left(a^{-\gamma} + K\sum_{i=1}^{n} x_i^{\gamma}\right)\right]}{n!\int_{\gamma_1}^{\gamma_2} \gamma^n a^{-\gamma} \prod_{i=1}^{n} x_i^{\gamma-1} \left(a^{-\gamma} + K\sum_{i=1}^{n} x_i^{\gamma}\right)^{-(n+1)} d\gamma}. \quad (21)$$

From Equation (20), we can calculate the expectations of x_R and γ as:

$$\mathrm{E}\{x_R \mid \underline{x}\} = \frac{I_3}{I_1}; \qquad \mathrm{E}\{\gamma \mid \underline{x}\} = \frac{I_2}{I_1}, \quad (22)$$

where

$$I_j = \int_{\gamma_1}^{\gamma_2} \gamma^{m_j} a^{-\gamma} \prod_{i=1}^{n} x_i^{\gamma-1} \left(a^{-\gamma} + K\sum_{i=1}^{n} x_i^{\gamma}\right)^{-(n+1)+k_j} \Gamma(n+1-k_j) d\gamma \quad j = 1, 2, 3,$$

with the following values of the parameters m_j and k_j:

$$m_1 \equiv m_3 = n; \quad m_2 = n+1; \quad k_1 \equiv k_2 = 0; \quad k_3 = 1/\gamma.$$

We can use the Equation (21) to get the center line from all the available data, and use a transformation, as follows,

$$z = x_R^{-\gamma}\left(a^{-\gamma} + K\sum_{i=1}^{n} x_i^{\gamma}\right), \quad (23)$$

to transform the random variable (x_R, γ) into a standard Gamma one. In this way, the Equation (20) of the probability density function can be transformed to

$$\text{pdf}\{z \mid \underline{x}\} = \frac{z^n \exp(-z)}{n!} = \frac{z^{(n+1)-1}}{\Gamma(n+1)} \exp(-z); \quad z \geq 0. \quad (24)$$

We can estimate the UCL and LCL of x_R control chart by inverse the Equation (22) as follows:

$$x_R = z^{-\frac{1}{\hat{\gamma}}}\left(a^{-\gamma} + K\sum_{i=1}^{n} x_i^{\gamma}\right)^{\frac{1}{\hat{\gamma}}}. \quad (25)$$

The Weibull control chart is more precise than the percentile-Weibull control chart and Bootstrap-Weibull control chart in control Weibull process because Erto and Pallotta (2007) had provided the sampling distribution of the control chart and exhibit the UCL and LCL of the control chart by using the sampling distribution.

The detection power of Erto's-Weibull control chart

Here, we use the Erto's-Weibull control chart to calculate the detection power under Bothe's capability adjustments for Weibull process. Let $X_1, X_2, \ldots, X_n$ be a sequence observation of independent and identically distributed in Weibull (α, γ). In order to compare with the detection power, we set the reliability level $R = 0.5$ be similar to the sampling distribution of $\overline{x}$, $\alpha = 1$ and $\gamma = 1\ (1)\ 10$, and we can compute the x_R from Equation (13). The interval (γ_1, γ_2) of the Uniform prior probability density function is set very close to the γ, and the number of subgroup is 100000. Tables 6 and 7 display the detection power of the Erto's-Weibull control chart when data comes from Weibull processes with right shifts and left shifts. The magnitude of shifts in the second column on the left is Bothe's capability adjustments are the same as in Tables 2 and 3. We can find that the detection power is almost more than 0.5, except $\gamma = 1$ and $n = 1, 2, 3, 4$. For example, when data comes from

Table 7. Detection power of the Erto's-Weibull control chart for $k < 0$ under various Weibull distributions.

n	Shift σ	Weibull distribution(1, γ) for left shift									
		γ=1	γ=2	γ=3	γ=4	γ=5	γ=6	γ=7	γ=8	γ=9	γ=10
2	2.12	0.985	0.971	0.972	0.978	0.98□	0.984	0.987	0.989	0.990	0.991
3	1.73	0.983	0.925	0.910	0.900	0.908	0.911	0.917	0.923	0.923	0.926
4	1.5	0.980	0.889	0.846	0.828	0.819	0.824	0.840	0.841	0.838	0.834
5	1.34	0.978	0.847	0.795	0.780	0.770	0.769	0.775	0.777	0.785	0.788
6	1.22	0.977	0.832	0.762	0.743	0.736	0.737	0.734	0.743	0.746	0.747
7	1.13	0.975	0.810	0.734	0.702	0.691	0.699	0.698	0.709	0.706	0.693
8	1.06	0.972	0.800	0.719	0.694	0.697	0.690	0.698	0.688	0.688	0.697
9	1.00	0.973	0.778	0.720	0.680	0.674	0.668	0.674	0.695	0.693	0.692
10	0.95	0.972	0.785	0.688	0.693	0.680	0.668	0.678	0.689	0.681	0.672

Weibull (1, 5) with right shift distance 1.5σ and subgroup size $n = 4$, the detection power of Erto's-Weibull control chart is 0.838>0.5. This means that the Bothe's adjustment is inadequate and will over-adjust the process capability.

DETECTION POWER COMPARISONS

Previously, we have introduced three control charts for Weibull processes, and we want to know which control chart is the most powerful in controling Weibull processes. Comparing the results in Tables 2 to 7, we find that, under the same mean shift adjustment, the detection power of the Erto's-Weibull control chart is the most powerful control chart for Weibull distributions. For example, when data comes from Weibull ($\alpha = 1,\ \gamma = 5$), and the subgroup size $n = 4$, the detection power of Erto's-Weibull control chart is (0.818) which is better than the detection power of percentile-Weibull control chart (0.699) and the detection power of bootstrap-Weibull control chart(0.617). Figures 1 and 2 display the power curve of the percentile-Weibull control chart (short-dotted line), the bootstrap-Weibull control chart (long-dotted line) and the Erto's-Weibull control chart (line) when data comes from Weibull ($\alpha = 1,\ \gamma = 1(1)10$) with right and left shifts and subgroup size $n = 2$. In the meantime, we also find that the power curve of the Erto's-Weibull control chart is almost on the left of the power curve of the other two control chart, except the shape parameter $\gamma > 6$ and the mean shifts are small. There are other power curves with subgroup sizes $n = 4 \text{ and } 6$ in Appendix.

CAPABILITY ADJUSTMENT

The index C_{pk} has been viewed as a yield-based index since it provides bounds on the process yield for a normality distributed process with a fixed value of C_{pk}. Given a fixed C_{pk} value, the production yield and fraction of defectives can be calculated (Table 8). Here, we adjust the formula of C_{pk} index to accommodate those shifts which can not be detected for the Weibull processes. Consequently, our adjustments provide much more accurate capability calculation for Weibull processes.

Estimator of C_{pk} in the non-normal case

In the recent years, several approaches of PCIs calculations for the non-normal processes have been suggested (Pal, 2005; Ding, 2004; Pearn and Chen, 1997; Kotz and Lovelace, 1998; Somerville and Montgomery, 1996; Kocherlakota and Kirmani, 1992; Clments, 1989; Shore, 1998). Chen and Pearn (1997) considered the generalizations of these basic capability indices to cover non-normal distribution. Since the median is usually the preferable central value for a skewed distribution, the index C_{pk} for non-normal processes called C_{Npk} were defined as follows

$$C_{Npk} = \min\left\{\frac{USL - M}{\left[\frac{F_{0.99865} - F_{0.00135}}{2}\right]}, \frac{M - LSL}{\left[\frac{F_{0.99865} - F_{0.00135}}{2}\right]}\right\}, \quad (26)$$

where $F_{0.00135}$ is the 0.135th percentile, $F_{0.99865}$ is the 99.865th percentile, and M is the median.

Modifying the assessment of C_{pk}

Since the mean shifts ranging in size from 0 up to

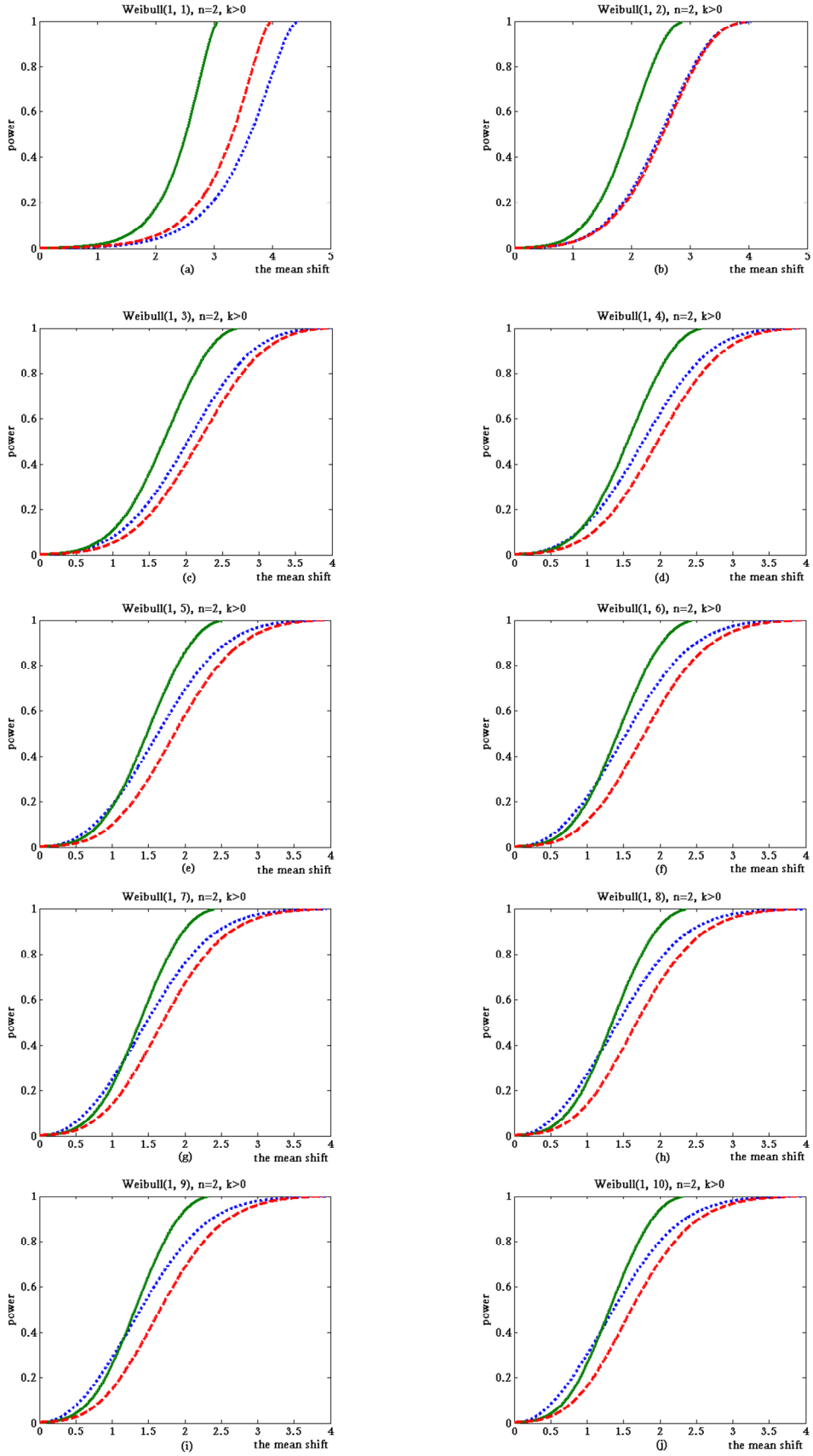

Figures 1. Power curve for subgroup size 2 when α=1, γ=1(1)10, $k > 0$.

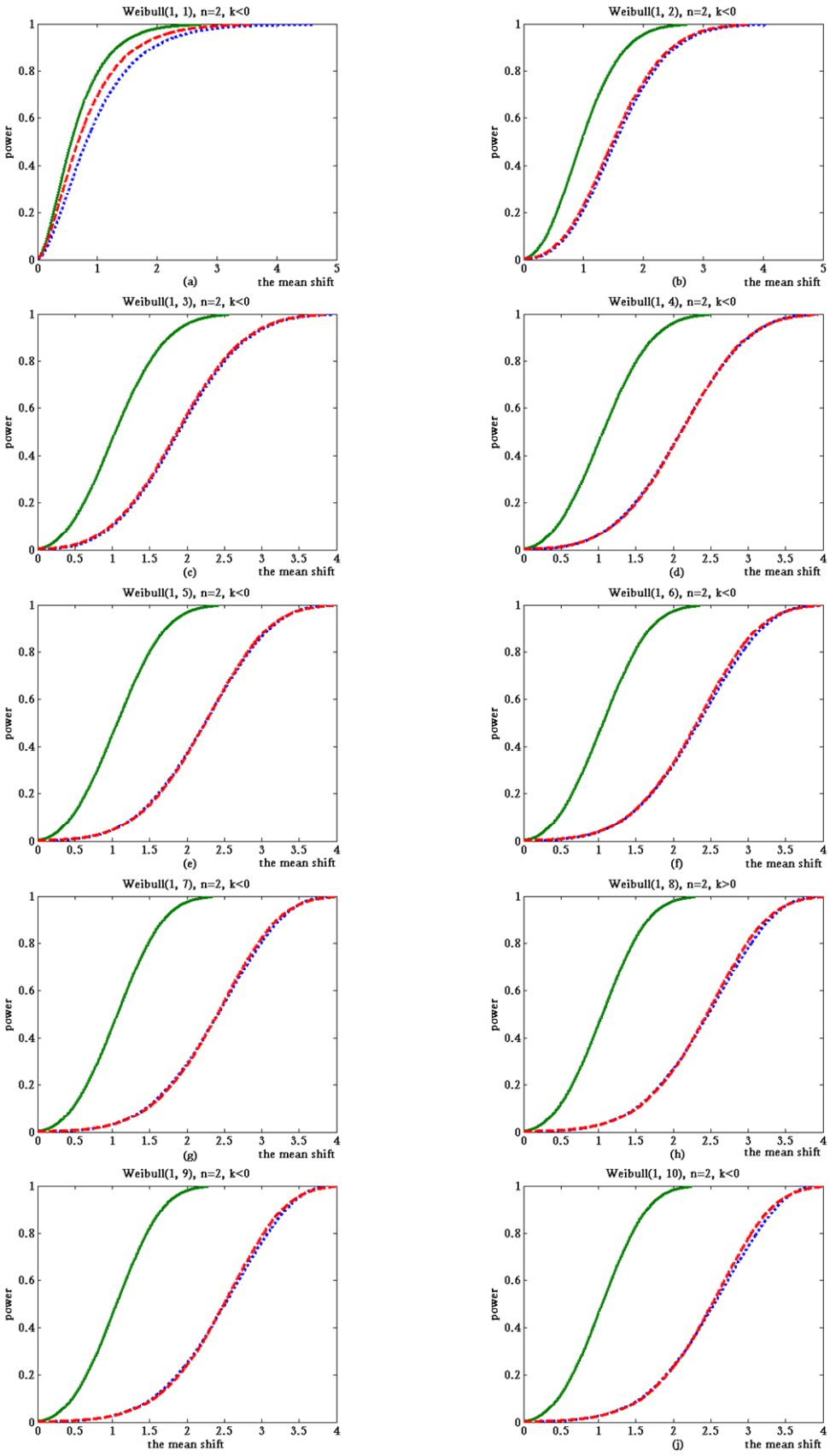

Figures 2. Power curve for subgroup size 2 when α=1, γ=1(1)10, $k < 0$.

Table 8. Some C_{pk} values versus the corresponding nonconformities.

C_{pk}	1	1.1	1.2	1.3	1.33	1.4	1.5	1.6	1.67	1.7	1.8	1.9
PPM	2699.796	966.848	318.217	96.193	66.073	26.691	6.795	1.587	0.544	0.34	0.067	0.012

$AS_{50}\sigma$ are likely to main undetected, a conservative method is to assume that every missed shift it as large as AS_{50}. We use M minus $AS_{50}\sigma$ to evaluate how well the process output meets the LSL and M plus $AS_{50}\sigma$ for determining conformance to the USL when estimating the index C_{pk}. Both of these adjustments are incorporated into the C_{pk} formula, which called the "dynamic" C_{Npk} index now, by making the following modifications,

$$dynamic\ C_{Npk} = \min\left\{\frac{USL-(M+AS_{50}\sigma)}{\left[\frac{F_{0.99865}-F_{0.00135}}{2}\right]}, \frac{(M-AS_{50}\sigma)-LSL}{\left[\frac{F_{0.99865}-F_{0.00135}}{2}\right]}\right\}$$

$$= \min\left\{\frac{USL-M-AS_{50}\sigma}{\left[\frac{F_{0.99865}-F_{0.00135}}{2}\right]}, \frac{M-AS_{50}\sigma-LSL}{\left[\frac{F_{0.99865}-F_{0.00135}}{2}\right]}\right\} \quad (27)$$

The AS_{50} have different results when the process distributions have right shifts or left shifts, but we can not know what sides the processes shift to. Since AS_{50} and C_{Npk} have an inverse ratio without being overestimated the process capability, to choose a larger AS_{50} is a better choice. Table 9 shows the larger AS_{50} when data comes from the same parameters with the subgroup size up to 30.

A procedure for calculating Weibull production yield with mean shift

Step 1

Give the sample size n, and parameters α and γ estimated by the maximum likelihood estimate (MLE) technique, and then obtain the mean shift adjustment, AS_{50}.

Step 2

Calculate the three quantiles $F_{0.00135}$, $F_{0.5}$, and $F_{0.99865}$ for $\sigma = \alpha^2[\Gamma(1+2\beta^{-1}) - \Gamma^2(1+\beta^{-1})]$ of the $\bar{X}_n$ ($\bar{X}_n = \frac{1}{n}\sum_{i=1}^{n} X_i$) distribution, where X_1, X_2, ..., X_n be sequence observations of independent and identically distributed in Weibull (α, γ).

Step 3

Calculate the estimated process capability C'_{npk} as follows $C'_{npk} = \min\left\{\frac{USL-F_{0.5}-AS_{50}\sigma}{F_{0.99865}-F_{0.5}}, \frac{F_{0.5}-AS_{50}\sigma-LSL}{F_{0.5}-F_{0.00135}}\right\}$ to assess the production yield and the practitioners can make reliable decisions to the process.

APPLICATION

Adjustable speed drives (ASDs) for medium and large size motors are increasingly being adopted for the automation, transportation, and control of industrial production. However, the usage of ASDs with ac induction motors has led to the premature failure of the winding insulation. The major reported failure occurs because of breakdown of the enameled wire insulation, and therefore, attraction of wire and motor manufacturers.

It has been observed that the failure of the inter-turn insulation is more likely due to the individual or combined effect of partial discharge (PD), dielectric heating, and space charge formation. Therefore, to survive in the inverter-fed motor environment, the insulation of magnet wire must have high resistance to PD, voltage overshoots, and high frequency components that can be above the discharge inception voltage.

Figure 3 shows the coating layers of magnet wire insulation and includes three layers (conductor, aromatic polyimide layer, PD resistant layer). Figure 4 is the pulse voltage test method for wire insulation. The voltage of the insulation aging test is from medium voltage (1.3 to 7.6 kV) pulse width modulated drives. For the circuit to safely and reliably operate at higher voltages, it utilizes a chain of insulated gate bipolar transistor (IGBT) switches connected in series. If there is a higher pulse voltage on test object, the surface of the insulation starts eroding and partial discharge. However, if the pulse voltage is over

Table 9. AS_{50} values for various subgroup sizes *n* and γ values of Weibull distribution(1, γ).

n \ γ	1	2	3	4	5	6	7	8	9	10
2	2.513	1.954	1.703	1.582	1.495	1.446	1.378	1.336	1.321	1.288
3	1.867	1.615	1.440	1.330	1.278	1.226	1.190	1.180	1.159	1.150
4	1.564	1.415	1.272	1.177	1.137	1.148	1.139	1.132	1.142	1.142
5	1.353	1.255	1.140	1.103	1.129	1.145	1.135	1.124	1.135	1.123
6	1.203	1.146	1.074	1.102	1.122	1.130	1.135	1.128	1.132	1.126
7	1.110	1.065	1.014	1.065	1.063	1.093	1.098	1.082	1.084	1.079
8	1.012	0.978	0.978	0.992	1.026	1.029	1.026	1.020	1.022	1.034
9	0.925	0.934	0.922	0.968	0.971	0.978	0.967	0.967	0.967	0.964
10	0.859	0.890	0.882	0.902	0.908	0.916	0.920	0.927	0.915	0.922
11	0.810	0.832	0.789	0.795	0.799	0.788	0.798	0.802	0.775	0.814
12	0.773	0.808	0.767	0.775	0.762	0.771	0.761	0.766	0.767	0.762
13	0.740	0.789	0.739	0.740	0.743	0.740	0.745	0.748	0.737	0.727
14	0.715	0.759	0.714	0.713	0.712	0.709	0.706	0.709	0.710	0.703
15	0.667	0.723	0.694	0.683	0.688	0.684	0.692	0.683	0.683	0.682
16	0.650	0.707	0.669	0.667	0.667	0.681	0.663	0.674	0.665	0.656
17	0.630	0.672	0.644	0.650	0.656	0.637	0.650	0.647	0.646	0.656
18	0.600	0.663	0.628	0.626	0.640	0.635	0.629	0.631	0.637	0.629
19	0.580	0.645	0.606	0.626	0.614	0.621	0.611	0.609	0.611	0.612
20	0.564	0.626	0.596	0.597	0.600	0.601	0.599	0.593	0.603	0.588
21	0.549	0.604	0.583	0.587	0.582	0.591	0.582	0.580	0.586	0.586
22	0.549	0.596	0.568	0.588	0.564	0.579	0.572	0.567	0.569	0.567
23	0.532	0.574	0.558	0.559	0.572	0.564	0.557	0.557	0.552	0.552
24	0.512	0.562	0.542	0.553	0.548	0.551	0.547	0.544	0.549	0.546
25	0.500	0.554	0.536	0.548	0.540	0.534	0.546	0.529	0.532	0.534
26	0.489	0.547	0.528	0.527	0.528	0.516	0.519	0.524	0.526	0.522
27	0.473	0.532	0.512	0.514	0.520	0.511	0.518	0.509	0.517	0.509
28	0.468	0.528	0.508	0.512	0.508	0.508	0.496	0.503	0.500	0.494
29	0.457	0.524	0.505	0.493	0.492	0.492	0.492	0.495	0.493	0.492
30	0.447	0.517	0.498	0.482	0.494	0.486	0.484	0.479	0.480	0.472

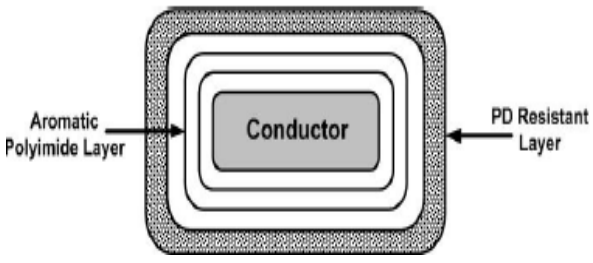

Figure 3. Coating layers of magnet wire insulation.

USL and the surface of the insulation starts eroding, the HV DC source would shutdown. The surface roughness as measured by a scanning electron microscope. Therefore, the *USL* and *LSL* for the voltage are 7.6 and 1.3 kV, respectively. As shown in Table 10, a part of historical data is collected. From Figures 5 and 6, we can

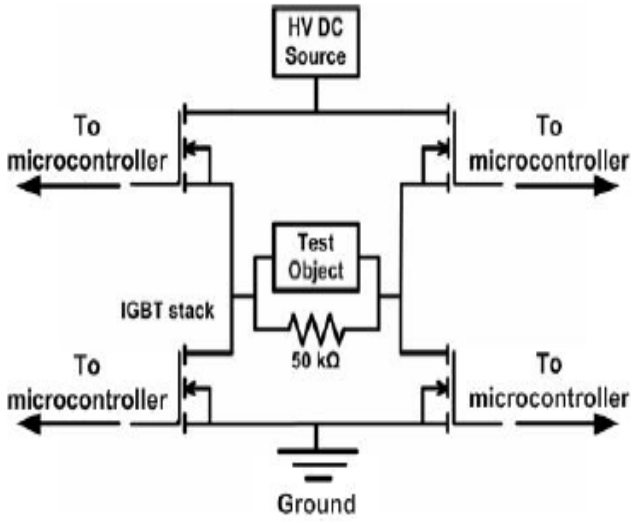

Figure 4. Pulse voltage test.

Table 10. The 100 observations are collected from the historical data.

5.992	5.371	4.413	2.486	4.348	3.991	2.892	4.921	4.857	5.051
4.508	4.695	5.368	4.897	4.245	5.273	5.137	4.746	3.124	1.783
5.707	4.374	5.463	4.893	4.145	5.208	4.896	4.065	3.507	4.512
5.933	5.514	5.456	3.107	4.099	5.156	2.830	2.288	4.488	4.501
4.541	5.219	2.514	5.119	4.558	5.895	4.497	4.973	4.627	5.783
4.537	2.876	4.141	3.628	4.201	4.390	5.208	5.050	3.765	4.686
4.207	4.097	4.368	3.986	4.528	4.665	5.112	5.229	3.807	3.479
4.062	3.525	3.872	4.223	4.170	4.964	3.728	5.360	4.184	4.368
4.989	3.102	5.470	5.730	4.522	4.153	3.308	2.583	4.456	4.890
5.269	4.507	2.978	3.503	4.935	3.896	3.394	4.900	4.103	2.379

conclude that the data collected from the factory are not distributed in normal. The results of data analysis justify that the process is significantly away from the normal distribution. By the goodness-of-fit tests, the historical data indicates that the process pretty approximates to be distributed as Weibull distribution. The parameters α and γ of this Weibull process could be estimated from the historical data, giving $\hat{\alpha}=4.797$ and $\hat{\gamma}=6$. Accordingly, it is appropriate to use this approach and we can obtain more accurate measures of the three quantiles, $F_{0.00135}$, M, and $F_{0.99865}$. In the meanwhile, σ can be calculated by Equation (8). Then, the dynamic C_{Npk} index of this process can be calculated as follows,

$$\begin{aligned} dynamic\ C_{Npk} &= \min\left\{\frac{USL-M-AS_{50}\sigma}{\left[\frac{F_{0.99865}-F_{0.00135}}{2}\right]}, \frac{M-AS_{50}\sigma-LSL}{\left[\frac{F_{0.99865}-F_{0.00135}}{2}\right]}\right\} \\ &= \min\left\{\frac{7.6\text{-}4.51\text{-}1.145(1.02)}{(7.08\text{-}1.29)/2}, \frac{4.51-1.145(1.02)-1.3}{(7.08\text{-}1.29)/2}\right\} \\ &= \min\{0.66, 0.71\} = 0.66, \end{aligned}$$

with AS_{50}=1.145 for n=5 from Table 9. Comparing it to the value of the following conventional index:

$$C_{Npk} = \min\left\{\frac{USL-M}{\left[\frac{F_{0.99865}-F_{0.00135}}{2}\right]}, \frac{M-LSL}{\left[\frac{F_{0.99865}-F_{0.00135}}{2}\right]}\right\} = \min\{1.07, 1.11\} = 1.07,$$

calculated by a traditional capability study (the shift of process mean is not considered), we can find that the value of the modified C_{Npk} is much smaller than the conventional index. This result indicated that if the process mean shifts are not detected, then the unadjusted C_{Npk} would overestimate the actual process yield which is not derisible. Our adjustment takes those shifts into account without being detected, so that the practitioner would be able to keep its quality promise for this process. As the adjusted process capability drops below the desired quality level, the practitioner should stop the process because the process does not meet his present capability requirement. As the subgroup size n increases, the shift in process mean has a higher probability of detection. An example in Table 9, if n=10, the value of AS_{50} would be 0.916 for Weibull (4.797, 6) and then the index of dynamic C_{Npk} is as below,

$$\begin{aligned} dynamic\ C_{Npk} &= \min\left\{\frac{USL-M-AS_{50}\sigma}{\left[\frac{F_{0.99865}-F_{0.135}}{2}\right]}, \frac{M-AS_{50}\sigma-LSL}{\left[\frac{F_{0.99865}-F_{0.00135}}{2}\right]}\right\} \\ &= \min\left\{\frac{7.6\text{-}4.51\text{-}0.916(1.02)}{(7.08\text{-}1.29)/2}, \frac{4.51-0.916(1.02)-1.3}{(7.08\text{-}1.29)/2}\right\} \\ &= \min\{0.74, 0.79\} = 0.74. \end{aligned}$$

The dynamic C_{Npk} will increase from 0.66 to 0.74 by changing n from 5 to 10, and the total number of nonconforming parts would be reduced.

Conclusion

In this paper, we considered the problem of how to determine the adjustments for process capability with mean shift when data follows the Weibull distribution. We first showed the detection powers of the percentile-Weibull control chart, bootstrap-Weibull control chart, and the Erto's-Weibull control chart under the Bothe's adjustments. We realized that the Bothe's adjustments are inadequate when data come from Weibull processes. After comparing the detection power, we found out that the Erto's-Weibull control chart is the most powerful control chart among the others for Weibull processes. Then we calculated the adjustments for

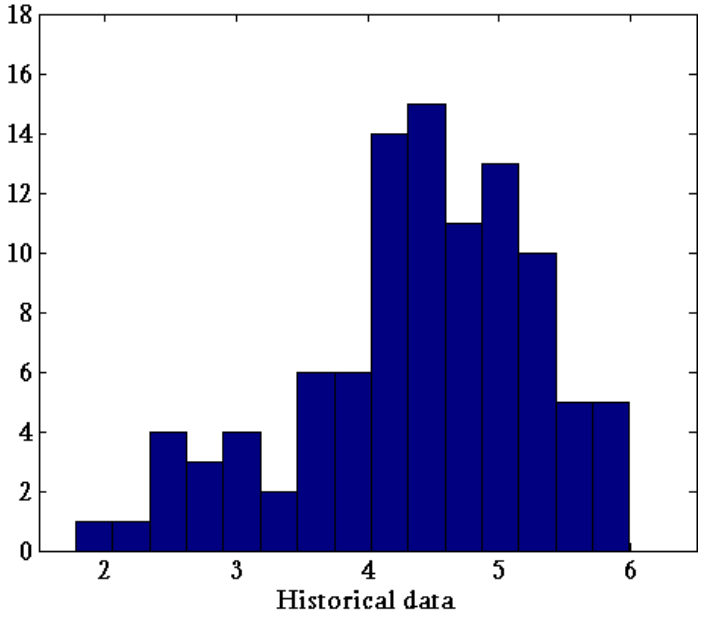

Figure 5. Histogram plot of the historical data.

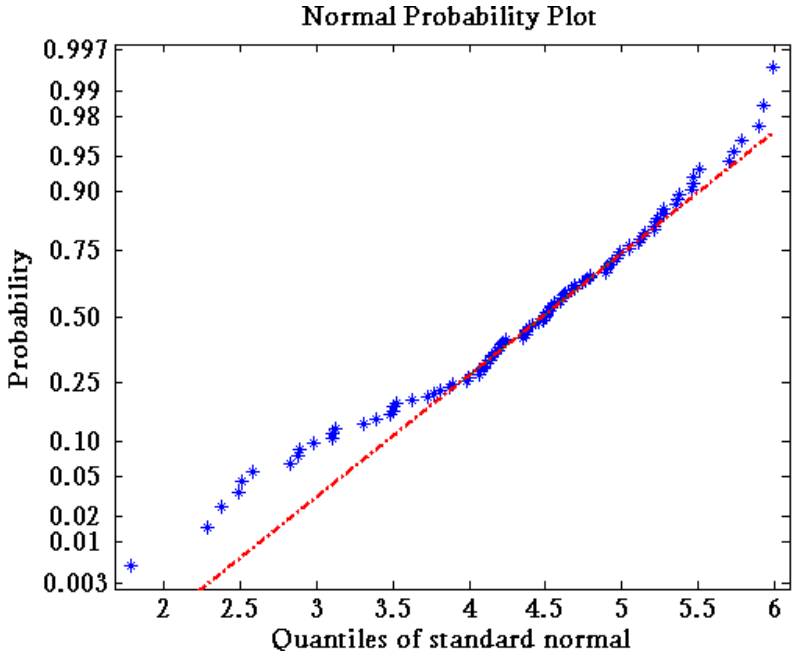

Figure 6. Normal probability plot of the historical data

various sample sizes (n) and Weibull shape parameter (γ) with detection power of the Erto's-Weibull control chart fixed to 0.5. Using the adjusted process capability formula, the engineers could determine the actual process capability more accurately. The tables were also provided for engineers or practitioners to use for their in-plant applications.

REFERENCES

Bender A (1975). Statistical tolerancing as it relates to quality control and the designer. Automotive Division Newsletter of ASQC.

Bothe DR (2002). Statistical reason for the 1.5σ shift. Qual. Eng., 14(3): 479-487.

Chan LK, Cheng SW and Spiring FA (1988). A new measure of process capability C_{pm}. J. Qual. Tech., 20(3): 162-175.

Chen KS. Pearn WL (1997). An application of non-normal process capability indices. Qual. Reliab. Eng. Int., 13: 355-360.
Choi KC, Nam KH, Park DH (1996). Estimation of capability index based on bootstrap method. Microelectron Reliab., 36(9): 141-153.
Clments JA (1989). Process capability calculations for non-normal distributions. Qual. Prog., September: 95-100.
Cygan P, Krishnakumar B, Laghari JR (1989). Lifetimes of polypropylene films under combined high electric field and thermal stresses. IEEE Trans. Electr. Insul., 24: 619-625.
Ding J (2004). A method of estimating the process capability index from the first four moments of non-normal data. Qual. Reliab. Eng. Int., 20: 787-805.
Erto P, Pallotta G (2007). A New Control Chart for Weibull Technological Processes. Qual. Tech. Quant. Manag., 4(4): 553-567.
Evans DH (1975). Statistical tolerancing: The state of the art, Part III: Shifts and Drifts. J. Qual. Tech., 7(2): 72-76.
Gilson JA (1951). New approach to engineering tolerances; Machinery Publishing Co., London.
Hsu YC, Pearn WL, Pei CW (2008). Capability adjustment for Gamma processes with mean shift consideration in implementing six sigma program. Eur. J. Oper. Res., 191(2): 517-529.
Kane VE (1986). Process capability indices. J Qual Tech. 18(1): 41-52.
Kocherlakota S, Kocherlakota K, Kirmani SNUA (1992). Process capability index under non-normality. Int. J. Math. Stat., 1(2): 175-210.
Kotz S, Lovelace CR (1998). Process capability indices in theory and practice. Arnold London, U. K.
Lu XM, Peng NF (2003). The approximation distribution for the sum of independent and identical Weibull distributions. National Chiao Tung University, Taiwan.
Nichols MD, Padgett WD (2006). A bootstrap control chart for Weibull percentiles. Qual. Reliab. Eng. Int., 22: 141-151.
Pal S (2005). Evaluation of non-normal process capability indices using generalized lambda distribution. Qual. Eng., 17: 77-85.
Pearn WL, Chen KS (1997). Capability indices for non-normal distributions with an application in electrolytic capacitor manufacturing. Microelectron. Reliab., 37(12): 1853-1858.
Pearn WL, Kotz S, Johnson NL (1992). Distributional and inferential properties of process capability indices. J. Qual. Tech., 24(4): 216-233.
Pyzdek T (1992). Process capability analysis using personal computers. Qual. Eng., 4(3): 419-440.
Shore H (1998). A new approach to analyzing non-normal quality data with application to process capability analysis. Int. J. Prod. Res., 36(7): 1917-1933.
Somerville SE, Montgomery DC (1996). Process capability indices and non-normal distributions. Qual. Eng., 9(2): 305-316.